Inorganic Chemistry

ARTICLE

pubs.acs.org/IC

Ultrafast Excited-State Dynamics of Rhenium(I) Photosensitizers $[Re(Cl)(CO)_3(N,N)]$ and $[Re(imidazole)(CO)_3(N,N)]^+$: Diimine Effects

Amal El Nahhas,[†] Cristina Consani,[†] Ana María Blanco-Rodríguez,[‡] Kyle M. Lancaster,[§,⊥] Olivier Braem,[†] Andrea Cannizzo,[†] Michael Towrie,[¶] Ian P. Clark,[¶] Stanislav Záliš,[*,∥] Majed Chergui,[*,†] and Antonín Vlček, Jr.[*,‡,∥]

[†]Laboratoire de Spectroscopie Ultrarapide, ISIC, FSB-BSP, Ecole Polytechnique Fédérale de Lausanne, CH-1015 Lausanne-Dorigny, Switzerland

[‡]School of Biological and Chemical Sciences, Queen Mary University of London, Mile End Road, London E1 4NS, United Kingdom

[⊥]Beckman Institute, California Institute of Technology, Pasadena, California 91125, United States

[¶]Central Laser Facility, STFC Rutherford Appleton Laboratory, Chilton, Didcot, Oxfordshire OX11 0QX, United Kingdom

[∥]J. Heyrovský Institute of Physical Chemistry, Academy of Sciences of the Czech Republic, Dolejškova 3, CZ-182 23 Prague, Czech Republic

Supporting Information

ABSTRACT: Femto- to picosecond excited-state dynamics of the complexes $[Re(L)(CO)_3(N,N)]^n$ (N,N = bpy, phen, 4,7-dimethyl-phen (dmp); L = Cl, n = 0; L = imidazole, n = 1+) were investigated using fluorescence up-conversion, transient absorption in the 650−285 nm range (using broad-band UV probe pulses around 300 nm) and picosecond time-resolved IR (TRIR) spectroscopy in the region of CO stretching vibrations. Optically populated singlet charge-transfer (CT) state(s) undergo femtosecond intersystem crossing to at least two hot triplet states with a rate that is faster in Cl $(\sim 100\ \text{fs})^{-1}$ than in imidazole $(\sim 150\ \text{fs})^{-1}$ complexes but essentially independent of the N,N ligand. TRIR spectra indicate the presence of two long-lived triplet states that are populated simultaneously and equilibrate in a few picoseconds. The minor state accounts for less than 20% of the relaxed excited population. UV−vis transient spectra were assigned using open-shell time-dependent density functional theory calculations on the lowest triplet CT state. Visible excited-state absorption originates mostly from mixed $L;N,N^{\bullet-} \rightarrow Re^{II}$ ligand-to-metal CT transitions. Excited bpy complexes show the characteristic sharp near-UV band (Cl, 373 nm; imH, 365 nm) due to two predominantly $\pi\pi^*(bpy^{\bullet-})$ transitions. For phen and dmp, the UV excited-state absorption occurs at ∼305 nm, originating from a series of mixed $\pi\pi^*$ and $Re \rightarrow CO;N,N^{\bullet-}$ MLCT transitions. UV−vis transient absorption features exhibit small intensity- and band-shape changes occurring with several lifetimes in the 1−5 ps range, while TRIR bands show small intensity changes (≤5 ps) and shifts (∼1 and 6−10 ps) to higher wavenumbers. These spectral changes are attributable to convoluted electronic and vibrational relaxation steps and equilibration between the two lowest triplets. Still slower changes (≥15 ps), manifested mostly by the excited-state UV band, probably involve local-solvent restructuring. Implications of the observed excited-state behavior for the development and use of Re-based sensitizers and probes are discussed.

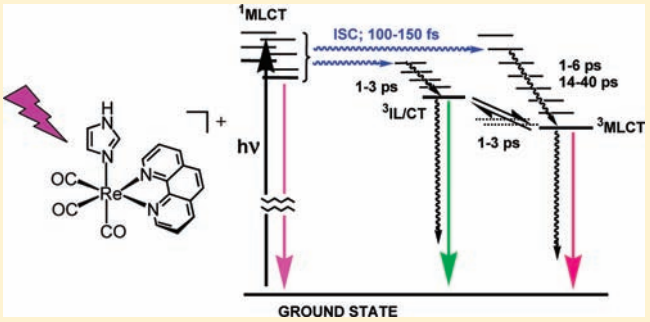

INTRODUCTION

Rhenium(I) carbonyldiimine complexes exhibit exceptionally rich excited-state behavior that can be tuned by structural variations and the medium.[1−3] They can be incorporated into a variety of environments, including supramolecules and polymers, or appended to biomolecules such as proteins or DNA. Strong photoluminescence and long-lived excited states with high reduction and oxidation potentials, together with synthetic flexibility and stability, make rhenium tricarbonyldiimines very convenient sensitizers[2,3] of electron-transfer (ET) and energy-transfer processes. They are also well suited for the photocatalysis of CO_2 reduction,[4−6] as phosphorescent labels and probes of biomolecules,[7−10] sensors,[11,12] or promising molecular switches[13−16] and organic light-emitting device emitters.[17] Electronically excited rhenium complexes have been used as IR probes of picosecond dynamics of dipolar solvents, ionic liquids, supramolecules, and proteins.[18−22] Their ability to trigger ultrafast ET has been demonstrated by a recent observation of a dramatic acceleration of long-range ET in Re-labeled azurin.[23,24]

Received: November 20, 2010
Published: March 09, 2011

Photonic functions of rhenium carbonyldiimines are, to a large extent, determined by their excited-state character and dynamics. These factors were studied in some depth[2,18,25,26] for complexes of the 2,2′-bipyridine ligand $[Re(L)(CO)_3(bpy)]^{n+}$. In short, allowed absorption to a singlet charge-transfer (^{1}CT) excited state involving a $Re(L)(CO)_3 \rightarrow$ bpy CT occurs between 340 and 420 nm. The optically prepared ^{1}CT state undergoes a ∼100 fs intersystem crossing (ISC), simultaneously populating an intermediate state, presumably a bpy-localized $\pi\pi^*$ intraligand (^{3}IL), and a vibrationally hot $Re(L)(CO)_3 \rightarrow$ bpy triplet CT (^{3}CT). The ^{3}IL to ^{3}CT conversion occurs on a 0.3−2 ps time scale, depending on the solvent and ligands.[25,26] The hot ^{3}CT state shows complex medium-sensitive relaxation dynamics on a time scale extending from units to hundreds of picoseconds or even early nanoseconds, depending on the medium.[18−22] The relaxed lowest ^{3}CT state then decays by minor radiative and major nonradiative pathways to the ground state, with the nonradiative decay being governed by the energy-gap law.[27,28]

Whereas the excited-state spectra, properties, and dynamics of $[Re(L)(CO)_3(bpy)]^{n+}$ are rather well understood, much less attention has been paid to their 1,10-phenanthroline analogues, $[Re(L)(CO)_3(phen)]^n$.[29−34] This lack of a fundamental understanding sharply contrasts with the much wider use of rhenium phenanthroline and, especially, methylphenanthroline complexes as sensitizers, phosphorescent labels, probes, sensors, switches, and ET phototriggers, stemming from their much longer excited-state lifetimes, higher emission quantum yields, and the availability of synthetic routes incorporating phen ligands into larger (supra)molecular constructs. In fact, there are reasons to expect significant differences in the early time excited-state behavior of bpy and phen complexes. Namely, the very nature of the lowest ^{3}CT state depends on the diimine ligand. Striplin and Crosby[33,34] have shown that the involvement of Re 5d orbitals, the metal-to-ligand CT (MLCT) character, and the spin−orbit (SO) coupling decrease in the order bpy > phen > dmp, presumably because of an increase in the IL($\pi\pi^*$) admixture to the ^{3}CT state.

Examining diimine ligand effects reveals factors controlling ISC and excited-state relaxation mechanisms in metal diimines, sheds more light on UV absorption and Raman spectra[35−37] of excited bpy and phen complexes, and directs the design of new Re-based sensitizers and their applications. In this study, we investigate femto- to picosecond time-resolved photoluminescence and UV−vis−IR transient absorption spectra of two series of complexes: $[Re(Cl)(CO)_3(N,N)]$ and $[Re(imH)(CO)_3(N,N)]^+$ (N,N = bpy, phen, dmp; imH = imidazole), with the latter being close models of protein-appended rhenium chromophores.[19,20,23,38−40] New aspects of the photophysics of rhenium tricarbonyldiimine complexes are revealed, especially the simultaneous population of two low-lying triplet states, lifetimes of the optically excited ^{1}CT states, and a multitude of picosecond electronic, vibrational, and solvation relaxation steps.

EXPERIMENTAL SECTION

Materials. $[Re(Cl)(CO)_3(N,N)]$ complexes were prepared using the literature procedure[29] and characterized by IR, ^{1}H NMR, and electrospray ionization mass spectrometry spectra.

$[Re(imH)(CO)_3(N,N)]NO_3$: A 100 mL round-bottomed flask was charged with $[Re(Cl)(CO)_3(N,N)]$ (0.5 mmol), silver triflate (0.5 mmol), and 40 mL of tetrahydrofuran. The reaction mixture was refluxed for 30 min. At this time, 5 mmol of imidazole was added and the reaction mixture refluxed for a further 2 h, then cooled to room temperature, and evaporated to dryness. The crude product was dry-packed onto a silica column. Following elution of a yellow impurity with MeCN, the column was washed with MeCN containing 20% water. A small yellow band preceded the product, which subsequently eluted as a substantial yellow band. The product fraction was collected and evaporated to dryness. The crude product was contaminated with imidazole, which was removed by dissolving the material in methanol and filtering. The filtrate was evaporated to dryness, dissolved in a minimal amount of boiling water, and precipitated with a saturated KNO_3 solution.

$[Re(CO_3)(phen)(imH)](NO_3)$: ^{1}H NMR (300 MHz, D_2O, solvent reference) δ 6.57 (s, 1H), 6.85 (s, 1H), 7.56 (s, 1H), 8.09 (dd, 2H, J = 6 and 9 Hz), 8.20 (s, 2H), 8.86 (d, 2H, J = 9 Hz), 9.65 (d, 2H, J = 4.5 Hz); IR (MeCN) ν(CO) 2032, 1924 (br) cm^{-1}. Elem anal. Calcd for $C_{18}H_{12}N_4O_3Re^+$ (M^+): m/z 518.5. Found: m/z 518.7.

$[Re(CO_3)(dmp)(imH)](NO_3)$: ^{1}H NMR (300 MHz, acetone-d_6, solvent reference) δ 3.05 (s, 6H), 6.67 (s, 1H), 6.97 (s, 1H), 7.64 (s, 1H), 8.11 (d, 2H, J = 6 Hz), 8.49 (s, 2H), 9.61 (d, 2H, J = 6 Hz); IR (MeCN) ν(CO) 2030, 1921 (br) cm^{-1}. Elem anal. Calcd for $C_{20}H_{16}N_4O_3Re^+$ (M^+): m/z 546.6. Found: m/z 546.7.

$[Re(CO_3)(bpy)(imH)](NO_3)$: ^{1}H NMR (300 MHz, acetone-d_6, solvent reference) δ 6.76 (s, 1H), 7.14 (s, 1H), 7.77 (s, 1H), 7.95 (t, 2H, J = 6 Hz), 8.46 (t, 2H, J = 7.5 Hz), 8.78 (d, 2H, J = 9 Hz), 9.40 (d, 2H, J = 6 Hz); IR (MeCN) ν(CO) 2032, 1924 (br) cm^{-1}. Elem anal. Calcd for $C_{16}H_{12}N_4O_3Re^+$ (M^+): m/z 494.5. Found: m/z 494.7

Spectroscopic measurements were performed in air-saturated *N*,*N*-dimethylformamide (DMF) of a spectroscopic quality (Aldrich). Solutions were placed in 0.5 mm quartz cells, and the sample concentrations for both transient absorption and up-conversion fluorescence experiments were adjusted to give absorbances of 0.2−0.3 at 400 nm.

Instruments. Time-resolved fluorescence spectra in the 440−680 nm range with a resolution of ∼130 fs were measured using the broad-band femtosecond fluorescence up-conversion setup described previously.[41,42] The samples were excited by 400 nm laser pulses, ∼100 fs (fwhm), ∼70 nJ per pulse, focused to a ∼50 μm (fwhm) spot, with a repetition rate of 250 kHz. The luminescence signal was mixed with a delayed 800 nm gate pulse. Spectra were corrected for the group velocity dispersion (GVD) but not for the spectral response of the detection system. Time zero was determined by detecting the up-converted Raman line of the solvent at 453 nm.

Time-resolved absorption (TA) spectra in the visible region were measured[43] using 400 nm pumping (∼100 fs, 1 kHz) and a white-light continuum probe beam (340−680 nm) that was generated by focusing a small part of the 800 nm fundamental output of the titanium sapphire (Ti:S) laser into a 1-mm-thick CaF_2 window. TA spectra in the deep-UV region were obtained using broad-band UV pulses generated by achromatic frequency doubling of a NOPA output.[44] Typically, samples were excited with 2 μJ at 400 nm (140 fs), focused on a spot of about 130 × 120 μm. The sample absorbance was 0.2−0.3 at 400 nm in a 0.2 mm flow cell. In both spectral regions, the relative polarization of the pump and probe light was set at the magic angle (54.7°). Intensities of the probe light transmitted by pumped and unpumped samples were recorded alternately by a 512-pixel silicon single-diode array using a mechanical chopper in the pump beam path. Spectra were GVD-corrected, and data obtained in the first 370−420 fs were removed to avoid contamination by the strong cross-phase-modulation signal from the solvent.

Time-Resolved IR (TRIR) Spectroscopy. The ULTRA instrument at the STFC Rutherford Appleton Laboratory was used and is described in detail elsewhere.[45] In brief, a Ti:S laser/regenerative amplifier (Thales) produces ∼50 fs pulses at a 10 kHz repetition rate. The laser output is split in two parts, one of which is frequency-doubled to 400 nm and used as a pump beam. The second pumps a TOPAS OPA, yielding signal and idler beams that are difference-frequency-mixed to

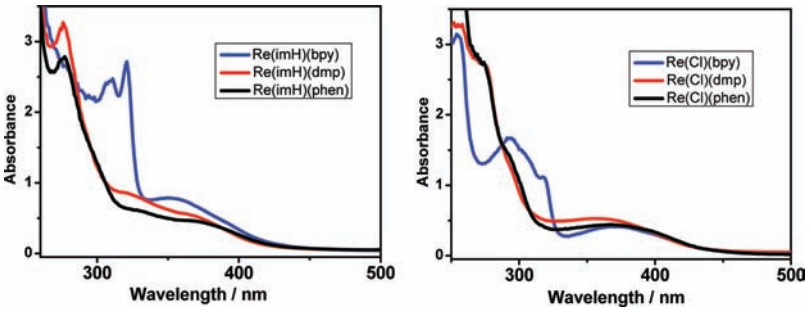

Figure 1. Absorption spectra of $[Re(imH)(CO)_3(N,N)]^+$ (left) and $[Re(Cl)(CO)_3(N,N)]$ (right) in DMF.

generate ~400 cm^{-1} broad mid-IR probe pulses. The mid-IR probe spectrum is recorded at a given time delay using two 128 element HgCdTe detectors (Infrared Associates). The sample is alternately pumped on and off to obtain difference absorption spectra. The sample solutions were flowed through a 0.1 mm CaF_2 cell that was simultaneously raster-scanned to avoid sample decomposition.

Fluorescence Up-Conversion and TA Data Analysis. Fluorescence up-conversion and TA experimental data were analyzed using singular value decomposition (SVD) to separate the stochastic noise from the signal $S(\lambda,t)$ and express the latter in terms of P spectral $\varepsilon_l(\lambda)$ and time $c_l(t)$ SVD components:

$$S(\lambda,t) = \sum_{l=1}^{P} \varepsilon_l(\lambda)\, c_l(t) \qquad (1)$$

Global fitting of the $c_l(t)$ components (kinetic vectors) to a multiexponential kinetic equation then provided lifetimes and corresponding noise-free decays associated spectra DAS.[25,26]

Kinetic equation (2) was used[25] to fit the fluorescence up-conversion data:

$$I(\lambda,t) = \{\mathrm{DAS}_1(\lambda)\, e^{-t/\tau_1} + \mathrm{DAS}_2(\lambda)\, e^{-t/\tau_2} + \mathrm{DAS}_{ph}(\lambda)\, [e^{-t/\tau_{ph}} - e^{-t/\tau_3}]\} \otimes e^{-(t/0.6\Delta_{IRF})^2} \qquad (2)$$

On the basis of our previous study of analogous bpy complexes,[25,26] we assume three characteristic emission decay times (τ_1, τ_2, and τ_{ph}) and a phosphorescence rise time τ_3 that is equal to τ_1. τ_{ph} stands for the 50−500 ns phosphorescence decay time that is effectively infinite on the present time scale. The last Gaussian term describes convolution with the instrument response function (IRF) of fwhm Δ_{IRF} = 100 fs.

For the TA data, the kinetic equation (3) was used:

$$\Delta A = \sum_{i=2} \mathrm{DAS}_i(\lambda)\, e^{-t/t_i} \otimes e^{-[(t-t_0)/0.6\Delta_{IRF}]^2} \qquad (3)$$

where the lifetimes are denoted as t_i. The cross-phase-modulation signals from the solvent extended for several hundreds of femtoseconds around the time zero, and the spectral region close to 400 nm was contaminated by scattered pump light. Therefore, the data obtained during the first 350 or 500 fs and between 390 and 410 nm were removed prior to the SVD analysis. Information on the TA of the optically populated singlet state and the t_1 ISC kinetics was thus lost. Depending on the rhenium complex, the sum (3) contains two or three terms, plus a final term corresponding to the nanosecond population decay, well beyond the experimental measurement range. This final summation term is called t_{inf}.

Quantum Chemical Calculations. The electronic structures of $[Re(L)(CO)_3(N,N)]^n$ (L = Cl or im; N,N = phen, dmp, bpy) were calculated by density functional theory (DFT) methods using the *Gaussian 09*[46] program package. DFT calculations employed Perdew, Burke, and Ernzerhof[47,48] (PBE0) hybrid functional. The solvent was described by the polarizable conductor continuum model (PCM).[49] The geometry of the lowest triplet state was calculated by the UKS approach. Low-lying triplet−triplet excitation energies were calculated by time-dependent DFT (TD-DFT) at the optimized triplet geometry. For H, C, N, O, and Cl atoms, either polarized triple-ζ basis sets 6-311g(d)[50,51] for geometry optimization and vibrational analysis or correlation consistent polarized valence double-ζ (cc-pvdz) basis sets[52] (TD-DFT) were used, together with quasi-relativistic effective-core pseudopotentials and a corresponding optimized set of basis functions for rhenium.[53,54] The simulation of optical spectra was performed using the *GaussSum*[55] software, including all calculated transitions and assuming Gaussian band shapes, 0.2 eV fwhm. The difference density plots were drawn using the *GaussView* software.

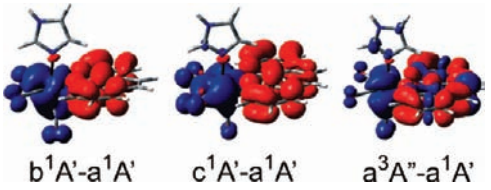

Figure 2. Difference electron density upon excitation from the a^1A ground state of $[Re(imH)(CO)_3(phen)]^+$ to the two lowest allowed singlet states (left, center) and to the lowest triplet state (right) at the ground-state geometry, determined with TD-DFT (PBE0/PCM-DMF) calculations. Regions of decreasing and increasing electron density are displayed in blue and red, respectively.

RESULTS

Steady-state absorption spectra of the investigated complexes $[Re(L)(CO)_3(N,N)]^n$ are shown in Figure 1. TD-DFT calculations (Table S1 in the Supporting Information) confirm the usual assignment[1−3,25,29,31,38,56−58] of the 350−420 nm absorption to several $Re(L)(CO)_3 \rightarrow N,N$ ^{1}CT transitions. (The notation used assumes C_s symmetry. The letters a, b, etc., denote the order of the states of given spin and symmetry.) Figure 2 shows the accompanying electron-density redistributions in $[Re(imH)(CO)_3(phen)]^+$ that manifest the predominant MLCT character of the lowest excited states, plus a minor imH → phen ligand-to-ligand CT (LLCT) contribution. The LLCT component is more pronounced for L = Cl.[25,56,57] Above the ^{1}CT transitions are strong bands of mostly $\pi\pi^*$ IL origin, which lie at higher energies in the case of phen/dmp complexes than in the case of bpy complexes. TD-DFT-calculated transitions to triplet states are summarized in Table S2 in the Supporting Information. The lowest triplet state a^3A'' calculated at the ground-state geometry has a mixed $Re(imH)(CO)_3 \rightarrow N,N/\pi\pi^*(N,N)$ character (Figure 2, right).

Fluorescence Up-Conversion. The temporal evolution of $[Re(L)(CO)_3(N,N)]^n$ photoluminescence is shown in Figure 3,

dx.doi.org/10.1021/ic102324p |*Inorg. Chem.* 2011, 50, 2932–2943

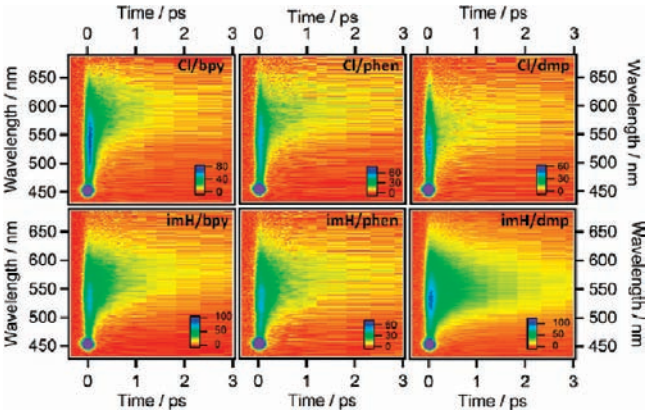

Figure 3. 2D plots of time-resolved luminescence spectra of $[Re(L)(CO)_3(N,N)]^n$ in DMF, measured after 400 nm, 100 fs excitation. Intensities are color-coded. The peak at 453 nm is the DMF Raman line.

using time−wavelength plots. Spectra measured at several fixed time delays are presented in Figure 4. A spectrally broad intense fluorescence peaking at 530−540 nm (Figure 3, blue region) emerges concomitantly with the excitation pulse. It is attributed[25,26] to the optically populated singlet excited state(s) of a $Re(L)(CO)_3 \rightarrow N,N$ CT origin. The fluorescence quickly evolves into a weak long-lived phosphorescence at slightly longer wavelengths that is identical with the stationary emission.

The temporal evolution of the luminescence spectra was analyzed by SVD. Kinetic $c_l(t)$ vectors (eq 1) were fitted using eq 2, which was previously found valid for $[Re(L)(CO)_3(bpy)]^n$ (L = halide, Etpy) photoluminescence.[25,26] Indeed, eq 2 provides satisfactory fits of the data, revealing that the fluorescence decays with two kinetic components for $[Re(Cl)(CO)_3(N,N)]$, $[Re(imH)(CO)_3(bpy)]^+$, and $[Re(imH)(CO)_3(phen)]^+$, whereas three components [adding a term $DAS_4(\lambda)\exp(-t/\tau_4)$] are required for $[Re(imH)(CO)_3(dmp)]^+$. The lifetime values are summarized in Table 1. Overlap of phosphorescence with the much stronger fluorescence prevents us from determining directly its rise time τ_3, whose value appears to be identical/close to τ_1.

Decay associated spectra (DAS) are shown in Figure 5. DAS_1, associated with the fluorescence decay τ_1, is the most intense, extending over the whole visible spectral region, up to at least 650 nm, peaking at ∼525 nm. DAS_2, attributed to the intermediate triplet state,[25,26] is much weaker and red-shifted to 550−590 nm. DAS_{ph}, due to the long-lived phosphorescence, is very weak and slightly (∼10 nm) red-shifted relative to DAS_2. DAS_4 of the extra decay component seen for $[Re(imH)(CO)_3(dmp)]^+$ nearly coincides in terms of wavelengths with DAS_{ph}.

To obtain more information on the triplet states and their dynamics, TA spectra in the IR, visible, and UV regions were investigated.

TRIR Spectra. TRIR spectra in the region of CO stretching vibrations, ν(CO), provide detailed information on the excited states of rhenium carbonyldiimines owing to their high sensitivity to electron-density distribution.[56,60,61] TRIR spectra of $[Re(Cl)(CO)_3(N,N)]$ (Figure 6) show three negative bands due to ground-state bleach and three positive bands, which are attributed[56,60−64] to a $Re(Cl)(CO)_3 \rightarrow N,N$ ^{3}CT excited state. Dynamic shifts to higher energies and shape changes of the excited-state bands taking place on a picosecond time scale are due to relaxation processes. The spectra were analyzed in the region of the highest band that corresponds to the totally symmetric in-phase ν(CO) vibration A′(1). Fitting to a sum of Gaussians (Figure 7) reveals the presence of two excited-state IR bands within the A′(1) envelope. The area of the minor band decreases over a few picoseconds to reach a constant value, accompanied by a commensurate rise in the major-band area (Figure S1 in the Supporting Information). The weaker band persists unchanged at 250−350 ps (Figure 7) when all of the relaxation processes are completed. [Another experiment (not shown) has confirmed its presence on a nanosecond time scale.] The final ratios of the two band areas are ca. 4:1 (bpy, phen) and 8:1 (dmp). It is proposed that two low-lying triplet excited states are populated simultaneously, entering a thermal equilibrium after a few picosecond relaxation period. The minor state should exhibit two more IR bands at lower energies, corresponding to A′(2) and A″ vibrations. Their presence is indeed manifested in the 1885−1925 cm^{-1} range by the bleach deepening (i.e., reaching more negative ΔAbs values) within the first 10 ps as the overlapping positive absorption decreases. Indeed, SVD/global-fitting analysis of this IR spectral region has identified a decaying component of the expected spectral shape that overlaps with the bleach (Figure 8).

To obtain information on the relaxation kinetics and the excited-state character, the time-dependent positions of the two A′(1) band maxima determined by the band-shape fitting were fitted to biexponential kinetics (Figure 9), producing two time constants of the dynamic band shift and the peak energies extrapolated to time infinity, when the relaxation processes are completed. The total shift of the major A′(1) band upon excitation was determined as a difference between this extrapolated A′(1) peak energy and the corresponding ground-state value. The shift magnitude, which qualitatively reports on the electronic depopulation of the $Re(Cl)(CO)_3$ moiety,[56,60,61] decreases in the order bpy (43.5) > phen (38.5) > dmp (31.4 cm^{-1}), indicating diminishing MLCT character of the lowest triplet state. This is most likely caused by an increase in the contribution of a N,N-localized IL $\pi\pi^*$ excitation to the lowest triplet state. The minor excited-state band is shifted from the ground-state A′(1) position less, by 30, 26, and 15 cm^{-1}, for bpy, phen, and dmp, respectively, indicating[61] that the corresponding excited state has less CT and more IL character than the major state. The kinetic parameters of the major-band upshift are summarized in the last two columns of Table 1, revealing ∼1 and 6−11 ps relaxation dynamics.

TA Spectra. Difference TA spectra of the $[Re(L)(CO)_3(N,N)]^n$ complexes are shown in Figures 10−12. The signal is positive across the UV and visible spectral regions, indicating that the excited-state absorption is much stronger than that of the ground state. Overlap with the bleach could distort slightly the shapes of the excited-state bands between 350 and 400 nm and below ∼300 nm (cf. Figure 1). Data obtained in the first 350 fs were removed to avoid contamination by cross-phase modulation and scattered pump light. TA spectra were thus measured at time delays longer than those of ISC and are attributed to the two triplet excited states, whose simultaneous presence was revealed by TRIR. Spectra of the two bpy complexes (Figure 10) display a typical[26] strong narrow band at 367 nm (L = imH) or 373 nm (L = Cl), which is due to a predominantly $\pi\pi^*$ IL transition of the $bpy^{\bullet-}$ ligand, followed by a group of weaker bands at ∼480 nm (L = Cl) or 425 and 451 nm (L = imH) attributed to L, $bpy^{\bullet-} \rightarrow Re^{II}(CO)_3$ LMCT transitions.[26] Spectra of the phen and dmp complexes

dx.doi.org/10.1021/ic102324p |Inorg. Chem. 2011, 50, 2932–2943

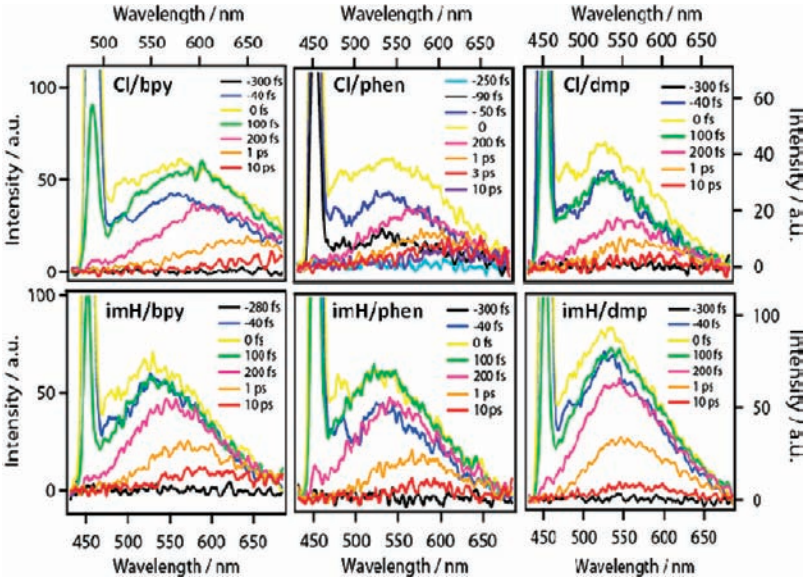

Figure 4. Luminescence spectra of $[Re(L)(CO)_3(N,N)]^n$ in DMF measured at selected time delays after 400 nm, 100 fs excitation. The peak at 453 nm is the DMF Raman line.

Table 1. Fluorescence (τ_i) and TA (t_i and t_i') Decay Lifetimes and TRIR Band-Shift Time Constants of $[Re(L)(CO)_3(N,N)]^{na}$

	fluorescence up-conversion			visible TA			UV TA			TRIR[b]	
complex	τ_1/fs	τ_2	τ_4	t_2	t_3	t_4	t_2'	t_3'	t_4'	shift$_1$	shift$_2$
Re(Cl)(bpy)[c]	97 ± 3	1.1 ± 0.1		3.3 ± 0.5	16 ± 3[d]		3.3 ± 0.5	16 ± 3[d]		1.1 ± 0.1[f]	11.0 ± 0.4[f]
Re(Cl)(phen)	108 ± 4	2.4 ± 0.3		2.5 ± 0.3	37 ± 11		1.0 ± 0.1	17 ± 3	72 ± 38	1.1 ± 0.1	8.5 ± 0.2
Re(Cl)(dmp)	110 ± 4	2.7 ± 0.4		3.6 ± 0.7	22 ± 9		1.1 ± 0.1	6.9 ± 1.5		1.0 ± 0.1	6.5 ± 0.6
Re(imH)(bpy)	150 ± 7	1.6 ± 0.2		1.9 ± 0.2	18 ± 4[d]		1.9 ± 0.2	18 ± 4[d]			
Re(imH)(phen)	144 ± 7	1.5 ± 0.2		3.9 ± 0.4	28 ± 6		2.0 ± 0.3	14 ± 2			
Re(imH)(dmp)	113 ± 5	0.9 ± 0.3	5.6 ± 2.4	1.1 ± 0.7	5 ± 2	30−60[e]	1.2 ± 1.1	5.5 ± 1.0	34 ± 11		

[a] Data are in picoseconds except τ_1. Measured in DMF unless stated otherwise. t_1 and t_1' lifetimes due to ISC are not reported because the first ~300 fs was omitted from the analysis. [b] In MeCN. [c] Data from ref 26. τ_1 and τ_2 values of 85 ± 8 fs and 0.34 ± 0.05 ps were measured in MeCN.[25] [d] Very low amplitude in the visible (t_3) but predominant in UV (373 and 366 nm for L = Cl and imH, respectively). [e] Low-amplitude component estimated from measurements over a 100 ps range. [f] 1.9 ± 0.1 and 9.4 ± 0.6 ps in DMF.[59]

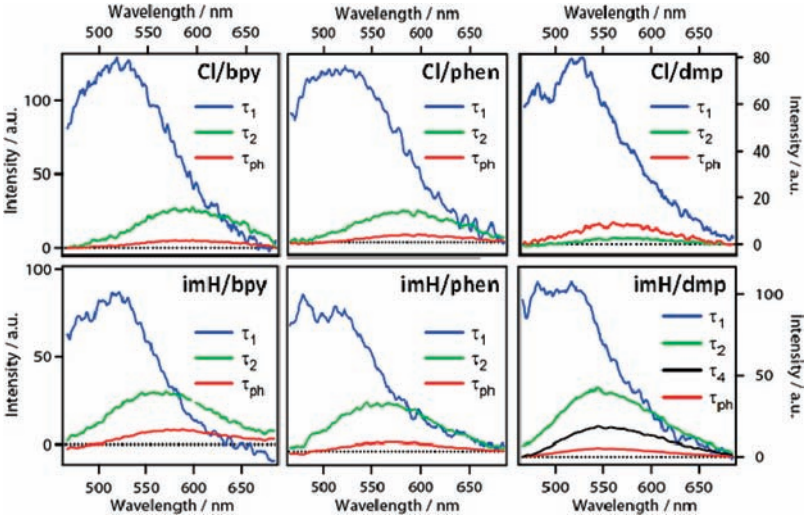

Figure 5. Luminescence DAS of $[Re(L)(CO)_3(N,N)]$ in DMF corresponding to fluorescence decay τ_1 (blue), intermediate state decay τ_2 (green), and phosphorescence decay τ_{ph} (red).

dx.doi.org/10.1021/ic102324p |*Inorg. Chem.* 2011, 50, 2932–2943

(Figure 11) also show a broad absorption between 450 and 600 nm, but the strong, sharp IL band in the near-UV spectral region is missing. Instead, an intense absorption band was found at ~305 nm using 400 nm pump/UV-broad-band probe spectroscopy (Figure 12). This band shifts slightly to lower energies and narrows upon a change of the axial ligand from Cl (307 nm; shoulders at 300 and 312 nm) to imH (304 nm; shoulders at 295, 301, and 307 nm). The observation of the ~305 nm UV band for $[Re(Cl)(CO)_3(phen)]$ agrees with a previous nanosecond experiment.[66] In the visible region, TA spectra of the phen and dmp complexes show a broad band at 470 and 565 (sh) nm (Cl, phen), 467 and 565 (sh) nm (Cl, dmp), 474 and 563 (sh) nm (imH, phen), and 466 and 568 (sh) nm (imH, dmp). These excited-state spectra broadly resemble the spectra of the corresponding reduced species;[66] for example, bands at 365 and 510 nm were reported for $[Re^{I}(Cl)(CO)_3(bpy^{\bullet-})]^{-}$ and at 550 and 590 nm for $[Re^{I}(Cl)(CO)_3(phen^{\bullet-})]^{-}$.

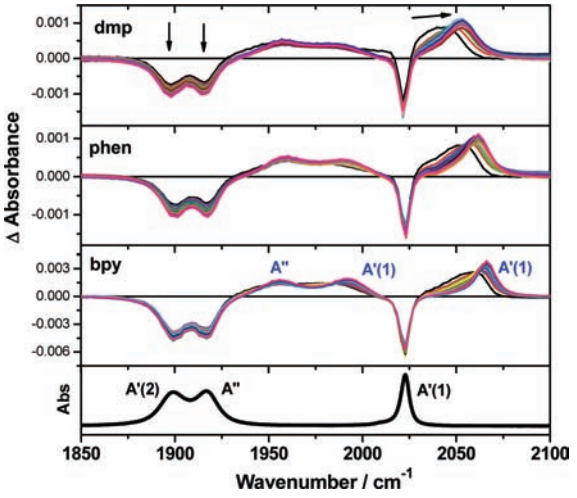

Figure 6. Difference TRIR spectra of $[Re(Cl)(CO)_3(N,N)]$ in MeCN measured after ~50 fs, 400 nm excitation over the time interval 1−250 ps. The time evolution is indicated by the arrows. Negative peaks correspond to the bleached ground state, and positive ones are due to the excited state(s). Spectral resolution: ~2 cm^{-1}. Bottom: ground-state FTIR spectrum of $[Re(Cl)(CO)_3(bpy)]$. Assignment from ref 65. A′(1), A′(2), and A″ are the totally symmetric in-phase, totally symmetric out-of-phase, and equatorial asymmetric CO stretching vibrations, respectively. Ground- and excited-state bands are labeled in black and blue, respectively.

UV−vis excited-state absorption features of the phen and dmp complexes were assigned using open-shell TD-DFT calculations of triplet−triplet transitions from the UKS-optimized lowest triplet state that, according to TRIR, amounts to ≥80% of the excited population. Characteristically for rhenium(I) tricarbonyldiimines,[25,56] DFT−UKS optimization identifies the

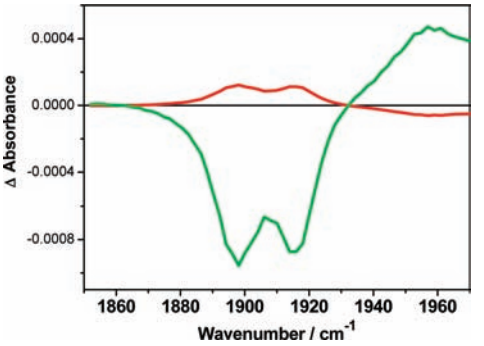

Figure 8. DAS obtained by SVD analysis of TRIR spectra of $[Re(Cl)(CO)_3(dmp)]$ in MeCN in the region of A″ and A′(2) vibrations. Green: time infinity corresponding to the long-time bleach recovery. Red: DAS corresponding to a 2.1 ± 1.5 ps kinetic component. The positive part reflects the transient spectrum due to the minor state whose decay is responsible for the early time bleach deepening, whereas the negative part between 1940 and 1960 cm^{-1} is due to the increasing A″ band of the major excited state.

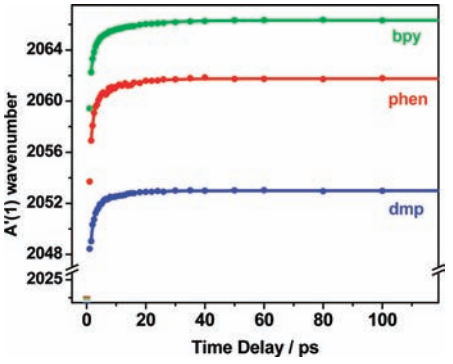

Figure 9. Time dependences of the peak wavenumbers of the major excited-state A′(1) IR band of $[Re(Cl)(CO)_3(N,N)]$. Fitted over a 1.5−350 ps range to biexponential kinetics. Ground-state peak positions are shown in the lower-left corner.

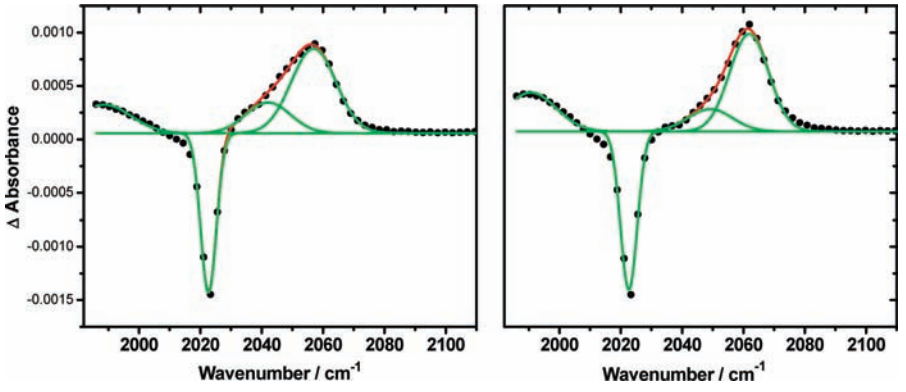

Figure 7. Gaussian analysis of the TRIR spectra of $[Re(Cl)(CO)_3(phen)]$ in MeCN recorded at 1.5 (left) and 250 ps (right) after ~50 fs, 400 nm excitation. Experimental points are shown in black, individual Gaussians in green, and their sums in red.

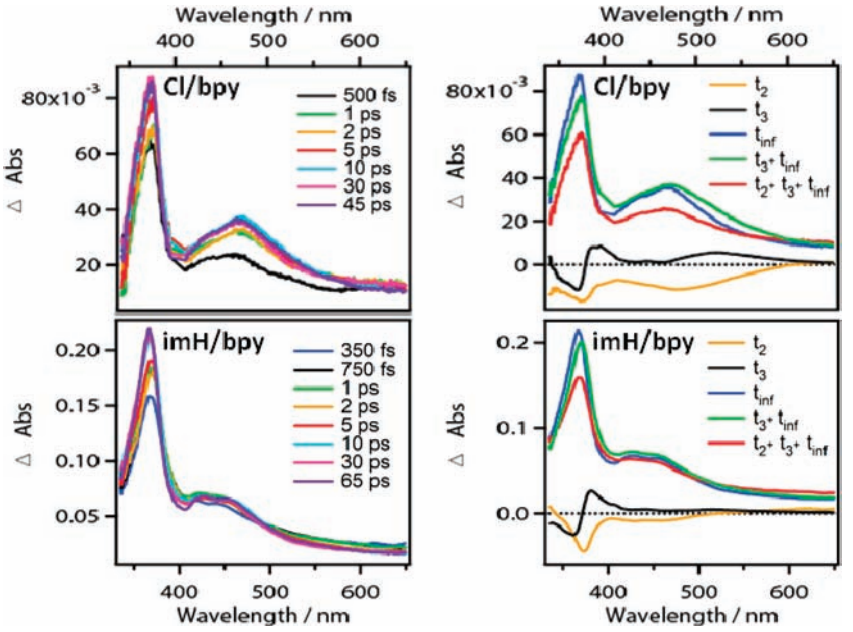

Figure 10. Left: TA spectra of $[Re(L)(CO)_3(bpy)]^n$ in DMF measured at selected time delays after 400 nm, ~120 fs excitation at a magic angle. The spectral region 390−410 nm is removed from the data. Right: DAS of $[Re(L)(CO)_3(bpy)]^n$ in DMF calculated from the TA spectra. t_{inf} corresponds to the nanosecond population decay. Top: L = Cl. Bottom: L = imH.

lowest triplet state as a^3A'' $Re(L)(CO)_3 \rightarrow N,N\ ^3CT$, assuming the C_s symmetry and neglecting the SO coupling. Symmetry-free calculations indicate that the C_s symmetry is lost on going to the lowest triplet state, with a^3A being thus a more appropriate notation. Hereafter, the discussion of transition energies, characters, and oscillator strengths is based on rigorous symmetry-free calculations, whereas the accompanying electron-density changes are shown assuming the C_s symmetry, for the sake of clarity. TD-DFT-calculated triplet−triplet transitions are summarized in Table S3 in the Supporting Information. As was found previously[26] for $[Re(L)(CO)_3(bpy)]^n$, the excited-state absorption in the visible spectral region results from $N,N^{\bullet-} \rightarrow Re^{II}(CO)_3$ and $L \rightarrow Re^{II}(CO)_3$ LMCT transitions, in some cases with smaller admixtures of $\pi\pi^*$ intra-$N,N^{\bullet-}$ excitations. Calculated UV excited-state spectra are shown in Figure 13. The peak maxima are blue-shifted by ca. 20 nm from the experimental values, while the essential spectral features are well reproduced, including the larger spectral width seen for $[Re(Cl)(CO)_3(dmp)]$ than $[Re(Cl)(CO)_3(phen)]$. It follows that, in the phen and dmp complexes, the UV excited-state absorption band originates from a series of intense electronic transitions, which have mixed $ML(CO)CT/\pi\pi^*$ and $\pi\pi^*/ML(N,N^{\bullet-})$ CT characters, where ML(CO)CT and $ML(N,N^{\bullet-})CT$ stand for $Re \rightarrow CO$ and $Re \rightarrow (N,N^{\bullet-})$ excitations (Figure S3 in the Supporting Information). The two strongest triplet−triplet transitions of $[Re(imH)(CO)_3(phen)]^+$ are visualized by electron-density changes depicted in Figure 14. The mixing between $\pi\pi^*(N,N^{\bullet-})$ and CT characters explains why the UV excited-state absorption is more affected by changing L from Cl to imH than by replacing phen with dmp. TD-DFT also reproduces (Figure S4 in the Supporting Information) the profound difference between the UV excited-state absorption spectra of phen/dmp and bpy complexes, whose strong near-UV band is due to two predominantly $\pi\pi^*(bpy^{\bullet-})$ transitions.

TA spectra display a picosecond time evolution that was analyzed by SVD and exponential global kinetic fitting to eq 3. The spectral changes can be best understood by comparing the raw spectra, DAS, and differences between the DAS sums. The DAS obtained for $[Re(imH)(CO)_3(bpy)]^+$ and $[Re(Cl)(CO)_3(bpy)]$ are very similar (Figure 10, right) and show a weak t_2 rise over the whole spectral region and a selective t_3 rise of the intense 373/367 nm band, accompanied by a small decrease on its low-energy side, around 380−390 nm. This behavior is typical of rhenium tricarbonylbipyridines.[26] UV and visible TA spectra of the phen and dmp complexes were measured and analyzed separately. In the visible region (Figure 11), the most prominent spectral changes occur on the units-of-picosecond time scale t_2. They are manifested by the growth of new absorption features on the red side of the ~470 nm band (500−600 nm) and around 350−370 nm. The ~470 nm band slightly decreases in intensity (L = Cl) or stays nearly constant (L = imH). The growing 500−600 nm absorption is much broader in the case of imH complexes, merging at longer time delays with the 470 nm feature into a single broad band. For L = Cl, the growing visible absorption manifests itself by distinct shoulders at ~520 and ~565 nm, which are much more intense in the case of $[Re(Cl)(CO)_3(phen)]$ than in the case of $[Re(Cl)(CO)_3(dmp)]$. The "slow" t_3 spectral changes occur with very low amplitudes and can be viewed as small band shifts or narrowing. More complex relaxation dynamics are manifested by the ~305 nm UV band (Figure 12). Both $[Re(Cl)(CO)_3(phen)]$ and $[Re(Cl)(CO)_3(dmp)]$ show a ~1 ps rise of the UV band, which is manifested by the t_2' DAS; see the blue curve in Figure 12. Narrowing and small blue shifts follow with time constants of 17 and 6.9 ps for phen and dmp, respectively. $[Re(Cl)(CO)_3(phen)]$ shows an additional ~70 ps low-amplitude decrease in intensity around the band maximum and at its blue side. The UV spectral changes of $[Re(Cl)(CO)_3(dmp)]$ occur (1.1 and 6.9 ps) with smaller amplitudes than those for $[Re(Cl)(CO)_3(phen)]$ and the slow (tens of picoseconds) component was not detected. The spectral time evolution is simpler for the imH complexes: the UV band grows in intensity

dx.doi.org/10.1021/ic102324p |*Inorg. Chem.* 2011, 50, 2932–2943

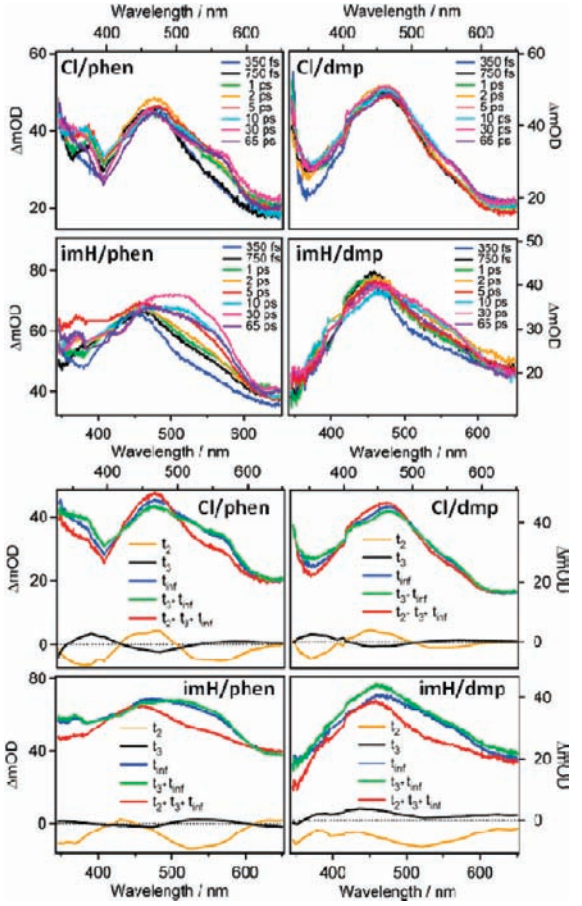

Figure 11. Top: Visible TA spectra of $[Re(L)(CO)_3(phen/dmp)]^n$ in DMF measured at selected time delays after 400 nm, ~120 fs excitation at magic angle. The spectral region 390−410 nm is removed from the data. Spectral intensities are normalized to the pump beam energy and absorbance of $[Re(imH)(CO)_3(dmp)]^+$. Bottom: DAS of $[Re(L)(CO)_3(phen/dmp)]^n$ in DMF calculated from the TA spectra. t_{inf} corresponds to the nanosecond population decay.

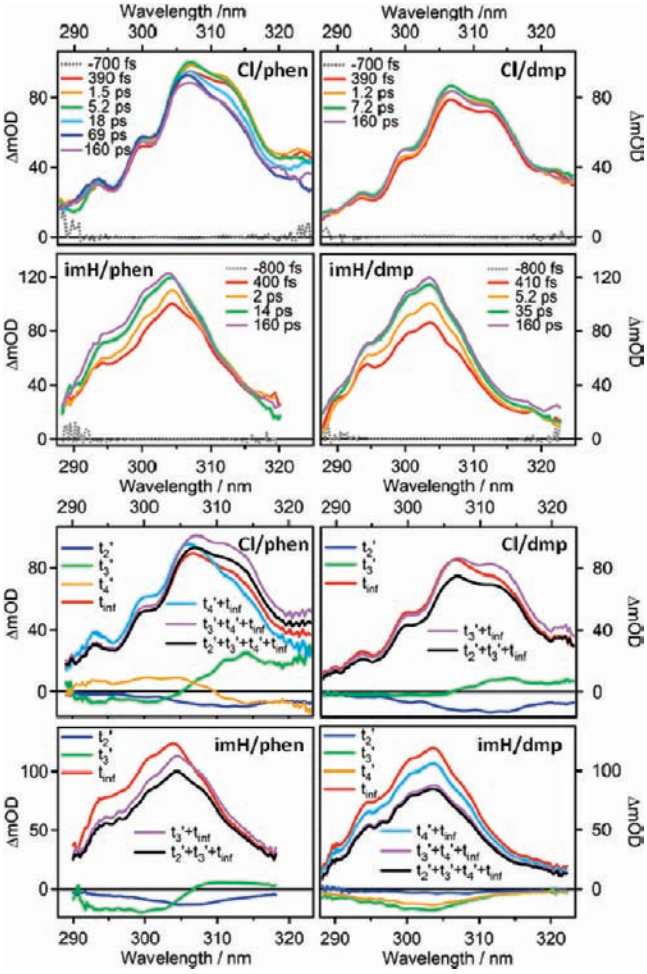

Figure 12. Top: UV TA spectra of $[Re(L)(CO)_3(phen/dmp)]^n$ in DMF measured at selected time delays after 400 nm, ~50 fs excitation at magic angle. Bottom: DAS of $[Re(L)(CO)_3(phen/dmp)]^n$ calculated from the time evolution of the TA spectra. t_{inf} corresponds to the nanosecond population decay. The bands are slightly skewed on their blue sides because of overlapping negative bleach (see Figure 1).

with time constants of 2 and 14 ps (phen) and 1.2, 5.5, and 34 ps (dmp). The 14 ps kinetics of $[Re(imH)(CO)_3(phen)]^+$ involves also narrowing of the red side of the band.

DISCUSSION

Experimental and theoretical results presented above allow us to develop the photophysical mechanism of $[Re(L)(CO)_3(N,N)]^n$ complexes (Scheme 1), assign excited-state spectral features ranging from deep UV to IR, and discuss ligand (L and N, N) effects on the ISC and relaxation dynamics. In the proposed interpretation, we stay within the limits of the spin-free model of singlet and triplet excited-state manifolds, considering SO coupling only as a perturbation allowing for ISC and triplet emission.[67] On the TD-DFT computational side, the spin-free approach allows us to optimize the lowest excited-state structure and calculate the triplet−triplet transitions.

The present spectroscopic results essentially confirm the photophysical mechanism that we proposed previously[25,26] for $[Re(L)(CO)_3(bpy)]^n$ complexes, although it is now necessary to consider the presence of the minor excited triplet state, equilibrated with the lowest-lying major one. The modified mechanism is shown in Scheme 1. This picture is still rather simplified because it does not consider all of the electronic states present and the SO coupling.[67] Time-resolved photoluminescence demonstrates that 400 nm excitation produces a fluorescent ^{1}CT state. Part of the excitation energy is lost during the first few tens of femtoseconds, as is documented by the "instantaneous" Stokes shift from 400 to ~530 nm. The optically populated ^{1}CT state decays on a femtosecond time scale (τ_1) into at least two triplet excited states: the long-lived phosphorescent a^3A'' lowest triplet and an intermediate triplet, presumably[25] b^3A''. Whereas τ_1 can be interpreted as the ^{1}CT lifetime (and, hence, the ISC time constant), τ_2 is probably a more complex kinetic parameter, related to lifetime(s) of the intermediate triplet state(s). For $[Re(imH)(CO)_3(dmp)]^+$, the spectra indicate the presence of another intermediate triplet, characterized by the τ_4 decay time. Both triplet states are initially formed hot, and the time evolution observed in the UV−vis and IR spectral region is attributed to their relaxation dynamics.

More detailed information on the triplets is provided by TRIR spectra, revealing a simultaneous subpicosecond population of two triplet excited states with different amounts of CT character. Their equilibration takes a few picoseconds at room temperature.

dx.doi.org/10.1021/ic102324p |*Inorg. Chem.* 2011, 50, 2932–2943

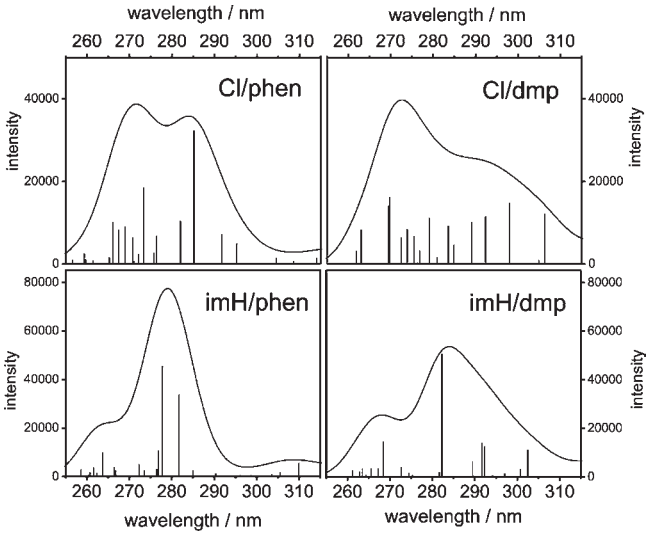

Figure 13. Simulated UV excited-state spectra and triplet−triplet electronic transitions (bars) of $[Re(L)(CO)_3(N,N)]^n$. TD-DFT (PBE0/CPCM-DMF) calculation on the a^3A state. Simulations include all transitions calculated in the 250−350 nm range; fwhm 0.2 eV.

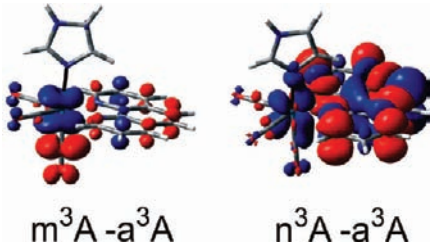

Figure 14. Electron-density changes upon the two strongest UV transitions from the lowest triplet state a^3A of $[Re(imH)(CO)_3(phen)]^+$ determined by TD-DFT (PBE0/PCM-DMF) calculations. Regions of decreasing and increasing electron density are displayed in blue and red, respectively. The transitions are described in Table S3 in the Supporting Information.

This conclusion, based on spectra of $[Re(Cl)(CO)_3(N,N)]$ in MeCN, can be extended to the whole family of rhenium tricarbonyldiimines because an asymmetric A′(1) band shape caused by two underlying excited-state ν(CO) bands has been observed (although not interpreted) for other complexes, including $[Re(imH)(CO)_3(phen)]^+$ in D_2O or appended to a protein surface,[19,20,58] $[Re(Cl)(CO)_3(bpy)]$ in a range of solvents,[59] or $[Re(Etpy)(CO)_3(bpy)]^+$ in ionic liquids.[21] The population ratio of the two states depends on the N,N and L ligands, as well as on the solvent and molecular environment of the rhenium chromophore. In the case of $[Re(Cl)(CO)_3(N,N)]$ in MeCN, the population ratio was estimated as the ratio of the corresponding A′(1) IR band areas, assuming that the two states have very similar IR molar absorptivities. The relative population of the minor state is about 20% for N,N = bpy and phen and ∼11% for N,N = dmp. The TRIR spectra confirm the assignment of the major state as a^3A'' of a predominantly $Re(CO)_3 \rightarrow$ N,N MLCT character, with the extent of Re/N,N charge separation decreasing in the order bpy > phen > dmp. The IL contribution is expected to increase in the same order. This conclusion agrees with the earlier observation that the zero-field splitting of the lowest triplet excited state decreases in the same order because of a decrease in the Re 5d contribution.[33,34] The minor excited state has less MLCT and more IL character, as is attested[61] by a smaller shift of ν(CO) vibrations upon excitation. Tentatively, it is assigned to b^3A'', i.e., the intermediate phosphorescent state. However, an alternative assignment to the highest SO component of the lowest triplet cannot be excluded.[67]

Scheme 1. Excited-State Relaxation Mechanism of $[Re(L)(CO)_3(N,N)]^n$ Complexes[a]

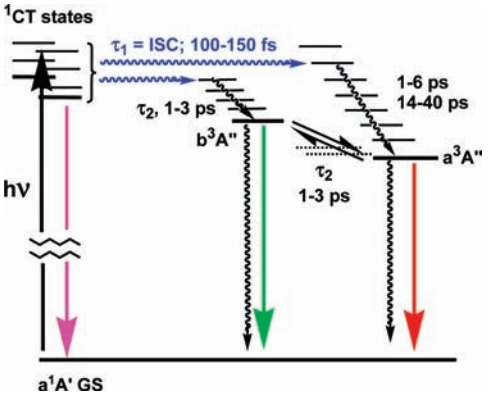

[a] Optical excitation populates at least two low-lying ^{1}CT states (Table S1 in the Supporting Information). Blue, violet, green, and red arrows denote the ISC, fluorescence, intermediate emission, and long-lived phosphorescence, respectively. ISC is assumed to populate $^3A''$ states only, based on symmetry arguments.[25] The actual density of states is much higher than that shown (Tables S1 and S2 in the Supporting Information): Several forbidden singlets and three of four triplets lie close to or below the optically populated ^{1}CT state. Inclusion of SO coupling produces at least 14 mixed-spin states in the relevant energy range,[67] which are schematically indicated by the dashed horizontal lines. The time constant (Table 1) τ_2 is pertinent mostly to the b^3A'' decay and relaxation; t_2 (t_2') is a convolution of intermediate and final triplet dynamics; t_3 and t_4 (t_3' and t_4') reflect mostly the final triplet relaxation. The observed equilibration could also involve the SO components of the lowest triplet.[67]

TA spectra in the visible region show a broad band around 500 nm that is assigned by open-shell triplet−triplet TD-DFT calculations to a group of L, $N,N^{\bullet-} \rightarrow Re^{II}$ LMCT transitions (Figure S3 in the Supporting Information) from the lowest MLCT triplet state a^3A'' that is approximately described as $*[Re^{II}(L)(CO)_3(N,N^{\bullet-})]^n$. Although some of these transitions are mixed with $\pi\pi^*(N,N^{\bullet-})$ excitations, TD-DFT predicts no intense predominantly $N,N^{\bullet-}$-localized $\pi\pi^*$ transitions in the visible range, implying that any similarity between the excited-state spectra and those of reduced $N,N^{\bullet-}$ ligands is largely coincidental. The same conclusion has been recently reached for analogous Re(bpy) complexes.[26] The main spectroscopic difference between the lowest excited state of $[Re(L)(CO)_3(bpy)]^n$ and the corresponding phen/dmp complexes occurs in the UV region. Whereas excited $[Re(L)(CO)_3(bpy)]^n$ shows a distinct sharp band at 373 nm (L = Br, Cl, and Etpy)[26] or 367 nm (imH) due to one or two strong transitions of predominantly $\pi\pi^*(bpy^{\bullet-})$ character,[26] $[Re(L)(CO)_3(phen/dmp)]^n$ complexes display a broader and more structured UV absorption band at shorter wavelengths, around 305 nm. This UV spectral feature arises from a series of mixed $\pi\pi^*$/MLCT transitions (see Figure 13 and Table S3 in the Supporting Information). The blue shift of the UV excited-state band on going from bpy to phen complexes parallels that observed for reduced complexes but not for the free ligands. For example,

dx.doi.org/10.1021/ic102324p |Inorg. Chem. 2011, 50, 2932–2943

whereas free $bpy^{\bullet-}$ to $phen^{\bullet-}$ shows an intense band at about the same wavelength of ~365 nm, the UV absorption of $[Cr(CO)_4(bpy^{\bullet-})]^-$ and $[W(CO)_4(phen^{\bullet-})]^-$ occurs at 375 nm and below 300 nm, respectively.[68,69]

Table 1 summarizes relaxation times determined by time-resolved spectroscopic experiments. The singlet-state lifetime τ_1 of $[Re(Cl)(CO)_3(N,N)]$ is essentially independent of the N,N ligand. On the other hand, changing the axial ligand from Cl to imH extends the singlet lifetime from ca. 100 to 150 fs for both bpy and phen. (The smaller value obtained for $[Re(imH)(CO)_3(dmp)]^+$ is hard to compare because of one more intermediate state involved and, hence, an additional ISC pathway.) The much larger effect of the axial ligand compared to the N,N ligand agrees with our previous observation[25] that the ISC rate is not influenced by small variations in the SO coupling energy, whereas metal−ligand (namely, Re−L) vibrational frequencies play an important role. τ_2 in the 1−3 ps range (and 5.4 ps τ_4 for $[Re(imH)(CO)_3(dmp)]^+$) cannot be directly identified with any elementary rate constant. According to Scheme 1, it results from convolution of ISC to the intermediate triplet(s), its vibrational relaxation, and equilibration with the lowest triplet. The latter process takes place (in MeCN) with subpicosecond and 2−5 ps time constants, as estimated by TRIR. The t_2 (1−4 ps) dynamics, pertinent to the TA spectral evolution in the visible region, seem to result mostly from equilibration of the two triplet states and their intramolecular vibrational energy redistribution/vibrational relaxation. (Note that vibrational relaxation of the lowest triplet does not contribute to the photoluminescence time τ_2, whereas it affects t_2.) The t_2' values determined for phen/dmp complexes in deep UV are comparable or slightly shorter than t_2 observed for the same compounds in the visible. The small differences could be explained assuming that the minor triplet contributes more to absorption in the visible region than in the UV region. The τ_4 (5−6 ps) value observed for $[Re(imH)(CO)_3(dmp)]^+$ has its counterparts in the visible, UV, and IR regions. It seems to originate mostly from conversion of an unidentified intermediate triplet state, which absorbs across the UV and visible regions, to the lowest triplet state. Finally, visible and UV excited-state absorption spectra show a long relaxation component t_4 (t_4'), in the tens of picosecond range. For bpy complexes,[18,26] it is manifested almost exclusively by the rise of the 373 nm band, with the spectral changes in the visible being negligible. Accordingly, we have found a ~18 ps rise of the 367 nm band in the case of $[Re(imH)(CO)_3(bpy)]^+$. The corresponding slow relaxation dynamics of phen and dmp complexes occur with smaller amplitudes across the whole UV−vis spectral region. They are most clearly manifested by the rise of the 304 nm band of $[Re(imH)(CO)_3(dmp)]^+$. In accordance with our previous hypothesis,[22,26] we tentatively attribute these "slow" dynamics to the later stages of vibrational relaxation and restructuring of the "local solvent", i.e., solvent molecules intercalated between the ligands of the excited rhenium chromophore. In reality, the "slow" relaxation is probably a complex multiphasic process and different spectroscopic transitions are differently sensitive to its components. This is probably why the slowest relaxation components measured in the IR are faster (~10 ps) than those in the UV−vis and why, in the case of phen/dmp complexes, the UV and visible relaxation dynamics are not always identical (Table 1).[70]

It has been noted many times that CT excited states of Ru^{II} and Re^{I} bpy complexes give much stronger resonance Raman (TR^3) signals than their phen analogues,[18,35−37,71] and these observations have led to a discussion[35−37] of possible differences in their excited-state character. Assuming that the excited-state Raman signals obtain their intensities from resonance with the intense UV electronic transition(s), it is possible to explain the higher Raman intensities of bpy complexes by the lower energies of their strong near-UV transitions, which lie closer to the Raman excitation wavelength (usually 400 or 355 nm) than in the case of their phen analogues, resulting in a larger enhancement.

Rhenium tricarbonylphenanthrolines are often preferred as photosensitizers and luminophores over analogous bipyridines because of their longer excited-state lifetimes and higher phosphorescence quantum yields, which both increase in the order bpy ≪ phen < dmp. Although these properties are pertinent to the relaxed lowest excited state only, the present ultrafast photophysical study also provides guidance for the design and application of Re-based sensitizers, probes, and phototriggers: (i) 100−150 fs singlet-state lifetimes are long enough to allow for ultrafast reactions of the optically populated ^{1}CT state. For example, subpicosecond ET occurs in a Re-labeled protein from a nearby tryptophan to an excited $[Re(imH)(CO)_3(dmp)]^+$,[23] and Re−C(ethyl) bond photolysis in $[Re(Et)(CO)_3(dmp)]$ is faster than 400 fs.[72,73] (ii) Both minor and major triplet excited states can undergo chemical reactions, such as ET. Although the energetics will be similar, the kinetics can differ because of different electron-density distributions in the two states, adding to the kinetic complexity.[23,24,74] (iii) Relaxation processes extend to a few tens of picoseconds in dipolar solvents and to a few nanoseconds in proteins[19,20] or ionic liquids.[21] Any excited-state reaction occurring on these time scales thus inevitably involves unequilibrated ("hot") states. (iv) Decreasing the charge separation in the lowest triplet in the order bpy > phen > dmp could affect the kinetics of excited-state ET reactions, although no experimental evidence is available yet. Relevant to photoinduced ET is the observation[75] of a relatively large spin density localized on the Me groups of the reduced $dmp^{\bullet-}$ ligand. Assuming similar localization of the excited electron in CT states of Re(dmp) chromophores, one can argue for the Me groups being involved in through-space intramolecular ET pathways. (v) CT excited states of $[Re(L)(CO)_3(N,N)]^n$ show UV−vis spectral features similar to those of their reduced forms $[Re(L)(CO)_3(N,N^{\bullet-})]^{n-1}$, making it hard to distinguish the two species and use UV−vis transient absorption to unravel the kinetics of photoinduced ET reactions. In any case, the observation of a strong UV absorption band (~370 and ~305 nm for bpy and phen, respectively) upon excitation of a diimine complex indicates the presence of a reduced $diimine^{\bullet-}$ ligand. (vii) $[Re(L)(CO)_3(N,N)]^n$ complexes can be used as TRIR probes of relaxation dynamics of dipolar solvents,[18,59] ionic liquids,[21] supramolecular media,[22] or proteins.[19,20,24] Because of the highly convoluted character of the processes occurring on time scales of up to ~10 ps, it seems that rhenium complexes would be most informative when probing slower relaxation processes, such as those observed in ionic liquids or proteins. As relaxation dynamics probes, bpy complexes should be superior to phen or dmp complexes because of a larger separation between the excited- and ground-state IR bands, more extensive Re/N,N charge transfer upon excitation, and smaller molecular size. On the other hand, phen and dmp complexes are a better choice as luminescence imaging agents and ET photosensitizers because of longer-lived and more emissive lowest excited states.

dx.doi.org/10.1021/ic102324p |Inorg. Chem. 2011, 50, 2932–2943

■ ASSOCIATED CONTENT

Supporting Information. Tables of TD-DFT-calculated singlet−singlet, singlet−triplet, and triplet−triplet transitions, figures showing the time dependence of major and minor excited-state A′(1) IR band areas of [Re(Cl)(CO)$_3$(dmp)], shapes of the relevant molecular orbitals of [Re(L)(CO)$_3$(N,N)]^n, and electron-density changes upon the three most intense triplet−triplet transitions of [Re(imH)(CO)$_3$(phen)]$^+$ occurring in the visible spectral region, and the full reference for the *Gaussian 09* software. This material is available free of charge via the Internet at http://pubs.acs.org.

■ AUTHOR INFORMATION

Corresponding Author

*E-mail: zalis@jh-inst.cas.cz (S.Z.), majed.chergui@epfl.ch (M.C.), a.vlcek@qmul.ac.uk (A.V.).

Present Addresses

§Department of Chemistry and Chemical Biology, Cornell University, Ithaca, NY 14853.

■ ACKNOWLEDGMENT

This work was supported by the Swiss NSF via the NCCR MUST, QMUL, European collaboration programs COST Action D35 and ESF-DYNA, STFC, and Czech Ministry of Education Grants ME10124 and LD11082. Work at Caltech was supported by GCEP (Stanford).

■ REFERENCES

(1) Stufkens, D. J.; Vlček, A., Jr. *Coord. Chem. Rev.* **1998**, *177*, 127.
(2) Vlček, A., Jr. *Top. Organomet. Chem.* **2010**, *29*, 73.
(3) Kumar, A.; Sun, S.-S.; Lees, A. J. *Top. Organomet. Chem.* **2010**, *29*, 1.
(4) Hawecker, J.; Lehn, J.-M.; Ziessel, R. *J. Chem. Soc., Chem. Commun.* **1983**, 536.
(5) Takeda, H.; Koike, K.; Inoue, H.; Ishitani, O. *J. Am. Chem. Soc.* **2008**, *130*, 2023.
(6) Takeda, H.; Ishitani, O. *Coord. Chem. Rev.* **2010**, *254*, 346–354.
(7) Lo, K. K.-W. *Top. Organomet. Chem.* **2010**, *29*, 115.
(8) Lo, K. K.-W.; Sze, K.-S.; Tsang, K. H.-K.; Zhu, N. *Organometallics* **2007**, *26*, 3440.
(9) Lo, K. K.-W.; Tsang, K. H.-K.; Sze, K.-S.; Chung, C.-K.; Lee, T. K.-M.; Zhang, K. Y.; Hui, W.-K.; Li, C.-K.; Lau, J. S.-Y.; Ng, D. C.-M.; Zhu, N. *Coord. Chem. Rev.* **2007**, *251*, 2292–2310.
(10) Lo, K. K.-W.; Louie, M.-W.; Zhang, K. Y. *Coord. Chem. Rev.* **2010**, *254*, 2603–2622.
(11) Peacock, A. F. A.; Batey, H. D.; Raendler, C.; Whitwood, A. C.; Perutz, R. N.; Duhme-Klair, A.-K. *Angew. Chem., Int. Ed.* **2005**, *44*, 1712–1714.
(12) Lewis, J. D.; Moore, J. N. *Dalton Trans.* **2004**, 1376.
(13) Ko, C.-C.; Kwok, W.-M.; Yam, V. W.-W.; Phillips, D. L. *Chem.—Eur. J.* **2006**, *12*, 5840.
(14) Patrocinio, A. O. T.; Iha, N. Y. M. *Inorg. Chem.* **2008**, *47*, 10851.
(15) Sarto Polo, A. S.; Itokazu, M. K.; Frin, K. M.; de Toledo Patrocinio, A. O.; Iha, N. Y. M. *Coord. Chem. Rev.* **2006**, *250*, 1669–1680.
(16) Beyeler, A.; Belser, P.; De Cola, L. *Angew. Chem., Int. Ed. Engl.* **1997**, *36*, 2779.
(17) Cleland, D. M.; Irwin, G.; Wagner, P.; Officer, D. L.; Gordon, K. C. *Chem.—Eur. J.* **2009**, *15*, 3682–3690.
(18) Liard, D. J.; Busby, M.; Matousek, P.; Towrie, M.; Vlček, A., Jr. *J. Phys. Chem. A* **2004**, *108*, 2363.
(19) Blanco-Rodríguez, A. M.; Busby, M.; Grădinaru, C.; Crane, B. R.; Di Bilio, A. J.; Matousek, P.; Towrie, M.; Leigh, B. S.; Richards, J. H.; Vlček, A., Jr.; Gray, H. B. *J. Am. Chem. Soc.* **2006**, *128*, 4365.
(20) Blanco-Rodríguez, A. M.; Busby, M.; Ronayne, K. L.; Towrie, M.; Sýkora, J.; Hof, M.; Záliš, S.; Grădinaru, C.; Di Bilio, A. J.; Crane, B. R.; Gray, H. B.; Vlček, A., Jr. *J. Am. Chem. Soc.* **2009**, *131*, 11788.
(21) Blanco-Rodríguez, A. M.; Ronayne, K. L.; Záliš, S.; Sýkora, J.; Hof, M.; Vlček, A., Jr. *J. Phys. Chem. A* **2008**, *112*, 3506.
(22) Blanco-Rodríguez, A. M.; Towrie, M.; Collin, J.-P.; Záliš, S.; Vlček, A., Jr. *Dalton Trans.* **2009**, 3941.
(23) Shih, C.; Museth, A. K.; Abrahamsson, M.; Blanco-Rodriguez, A. M.; Di Bilio, A. J.; Sudhamsu, J.; Crane, B. R.; Ronayne, K. L.; Towrie, M.; Vlček, A., Jr.; Richards, J. H.; Winkler, J. R.; Gray, H. B. *Science* **2008**, *320*, 1760.
(24) Blanco-Rodríguez, A. M.; Di Bilio, A. J.; Shih, C.; Museth, A. K.; Clark, I. P.; Towrie, M.; Cannizzo, A.; Sudhamsu, J.; Crane, B. R.; Sýkora, J.; Winkler, J. R.; Gray, H. B.; Záliš, S.; Vlček, A. *Chem.—Eur. J.* **2011**, in press.
(25) Cannizzo, A.; Blanco-Rodríguez, A. M.; Nahhas, A.; Šebera, J.; Záliš, S.; Vlček, A., Jr.; Chergui, M. *J. Am. Chem. Soc.* **2008**, *130*, 8967.
(26) El Nahhas, A.; Cannizzo, A.; van Mourik, F.; Blanco-Rodríguez, A. M.; Záliš, S.; Vlček, A., Jr.; Chergui, M. *J. Phys. Chem. A* **2010**, *114*, 6361.
(27) Worl, L. A.; Duesing, R.; Chen, P.; Della Ciana, L.; Meyer, T. J. *J. Chem. Soc., Dalton Trans.* **1991**, 849.
(28) Hino, J. K.; Della Ciana, L.; Dressick, W. J.; Sullivan, B. P. *Inorg. Chem.* **1992**, *31*, 1072.
(29) Wrighton, M. S.; Morse, D. L. *J. Am. Chem. Soc.* **1974**, *96*, 998.
(30) Fredericks, S. M.; Luong, J. C.; Wrighton, M. S. *J. Am. Chem. Soc.* **1979**, *101*, 7415.
(31) Wallace, L.; Rillema, D. P. *Inorg. Chem.* **1993**, *32*, 3836.
(32) Wallace, L.; Jackman, D. C.; Rillema, D. P.; Merkert, J. W. *Inorg. Chem.* **1995**, *34*, 5210.
(33) Striplin, D. R.; Crosby, G. A. *Chem. Phys. Lett.* **1994**, *221*, 426.
(34) Striplin, D. R.; Crosby, G. A. *Coord. Chem. Rev.* **2001**, *211*, 163.
(35) Kumar, C. V.; Barton, J. K.; Turro, N. J.; Gould, I. R. *Inorg. Chem.* **1987**, *26*, 1455.
(36) Turró, C.; Chung, Y. C.; Leventis, N.; Kuchenmeister, M. E.; Wagner, P. J.; Leroi, G. E. *Inorg. Chem.* **1996**, *35*, 5104.
(37) Schoonover, J. R.; Omberg, K. M.; Moss, J. A.; Bernhard, S.; Malueg, V. J.; Woodruff, W. H.; Meyer, T. J. *Inorg. Chem.* **1998**, *37*, 2585.
(38) Connick, W. B.; Di Bilio, A. J.; Hill, M. G.; Winkler, J. R.; Gray, H. B. *Inorg. Chim. Acta* **1995**, *240*, 169.
(39) Di Bilio, A. J.; Crane, B. R.; Wehbi, W. A.; Kiser, C. N.; Abu-Omar, M. M.; Carlos, R. M.; Richards, J. H.; Winkler, J. R.; Gray, H. B. *J. Am. Chem. Soc.* **2001**, *123*, 3181.
(40) Crane, B. R.; Di Bilio, A. J.; Winkler, J. R.; Gray, H. B. *J. Am. Chem. Soc.* **2001**, *123*, 11623.
(41) Cannizzo, A.; van Mourik, F.; Gawelda, W.; Zgrablic, G.; Bressler, C.; Chergui, M. *Angew. Chem., Int. Ed.* **2006**, *45*, 3174.
(42) Zgrablić, G.; Voitchovsky, K.; Kindermann, M.; Haacke, S.; Chergui, M. *Biophys. J.* **2005**, *88*, 2779.
(43) Helbing, J.; Bonacina, L.; Pietri, R.; Bredenbeck, J.; Hamm, P.; van Mourik, F.; Chaussard, F.; Gonzalez-Gonzalez, A.; Chergui, M.; Ramos-Alvarez, C.; Ruiz, C.; Lopez-Garriga, J. *Biophys. J.* **2004**, 87.
(44) Consani, C.; Mirabelle Prémont-Schwarz, M.; El Nahhas, A.; Bressler, C.; van Mourik, F.; Cannizzo, A.; Chergui, M. *Angew. Chem., Int. Ed.* **2009**, *48*, 7184–7187.
(45) Greetham, G.; Burgos, P.; Cao, Q.; Clark, I. P.; Codd, P.; Farrow, R.; George, M. W.; Kogimtzis, M.; Matousek, P.; Parker, A. W.; Pollard, M.; Robinson, D.; Xin, Z.-J.; Towrie, M. *Appl. Spectrosc.* **2010**, *64*, 1311.
(46) Frisch, M. J. et al. *Gaussian 09*, revision A.02; Gaussian, Inc.: Wallingford, CT, 2009.
(47) Perdew, J. P.; Burke, K.; Ernzerhof, M. *Phys. Rev. Lett.* **1996**, *77*, 3865.
(48) Adamo, C.; Barone, V. *J. Chem. Phys.* **1999**, *110*, 6158.

(49) Tomasi, J.; Mennucci, B.; Cammi, R. *Chem. Rev.* **2005**, *105*, 2999.
(50) Raghavachari, K.; Binkley, J. S.; Seeger, R.; Pople, J. A. *J. Chem. Phys.* **1980**, *72*, 650.
(51) Curtiss, L. A.; McGrath, M. P.; Blaudeau, J.-P.; Davis, N. E.; Binning, R. C., Jr.; Radom, L. *J. Chem. Phys.* **1995**, *103*, 6104.
(52) Woon, D. E.; Dunning, T. H., Jr. *J. Chem. Phys.* **1993**, *98*, 1358.
(53) Andrae, D.; Häussermann, U.; Dolg, M.; Stoll, H.; Preuss, H. *Theor. Chim. Acta* **1990**, *77*, 123.
(54) Martin, J. M. L.; Sundermann, A. *J. Chem. Phys.* **2001**, *114*, 3408.
(55) O'Boyle, N. M.; Tenderholt, A. L.; Langner, K. M. *J. Comput. Chem.* **2008**, *29*, 839.
(56) Vlček, A., Jr.; Záliš, S. *Coord. Chem. Rev.* **2007**, *251*, 258.
(57) Vlček, A., Jr.; Záliš, S. *J. Phys. Chem. A* **2005**, *109*, 2991.
(58) Busby, M.; Gabrielsson, A.; Matousek, P.; Towrie, M.; Di Bilio, A. J.; Gray, H. B.; Vlček, A., Jr. *Inorg. Chem.* **2004**, *43*, 4994.
(59) Blanco-Rodríguez, A. M.; Towrie, M.; Clark, I. P.; Záliš, S.; Vlček, A., Jr. Manuscript in preparation.
(60) Dattelbaum, D. M.; Omberg, K. M.; Schoonover, J. R.; Martin, R. L.; Meyer, T. J. *Inorg. Chem.* **2002**, *41*, 6071.
(61) Dattelbaum, D. M.; Omberg, K. M.; Hay, P. J.; Gebhart, N. L.; Martin, R. L.; Schoonover, J. R.; Meyer, T. J. *J. Phys. Chem. A* **2004**, *108*, 3527.
(62) George, M. W.; Johnson, F. P. A.; Westwell, J. R.; Hodges, P. M.; Turner, J. J. *J. Chem. Soc., Dalton Trans.* **1993**, 2977.
(63) Gamelin, D. R.; George, M. W.; Glyn, P.; Grevels, F.-W.; Johnson, F. P. A.; Klotzbücher, W.; Morrison, S. L.; Russell, G.; Schaffner, K.; Turner, J. J. *Inorg. Chem.* **1994**, *33*, 3246.
(64) Dattelbaum, D. M.; Martin, R. L.; Schoonover, J. R.; Meyer, T. J. *J. Phys. Chem. A* **2004**, *108*, 3518.
(65) Bredenbeck, J.; Helbing, J.; Hamm, P. *J. Am. Chem. Soc.* **2004**, *126*, 990.
(66) Kalyanasundaram, K. *J. Chem. Soc., Faraday Trans. 2* **1986**, *82*, 2401.
(67) Baková, R.; Chergui, M.; Daniel, C.; Vlček, A., Jr.; Záliš, S. *Coord. Chem. Rev.* **2011**, *255*, 975.
(68) Víchová, J.; Hartl, F.; Vlček, A., Jr. *J. Am. Chem. Soc.* **1992**, *114*, 10903.
(69) Lindsay, E.; Vlček, A., Jr.; Langford, C. H. *Inorg. Chem.* **1993**, *32*, 2269.
(70) A very good correspondence between luminescence, UV, and visible absorption was found for $[Re(imH)(CO)_3(dmp)]^+$. The 37 ps relaxation time of $[Re(Cl)(CO)_3(phen)]$ determined in the visible region has a very small associated amplitude. It could be an average of the 17 and 72 ps time constants that are better resolved in the deep-UV region. On the other hand, the UV relaxation times of $[Re(Cl)(CO)_3(dmp)]$ and $[Re(imH)(CO)_3(dmp)]^+$ are faster than the visible ones.
(71) Smothers, W. K.; Wrighton, M. S. *J. Am. Chem. Soc.* **1983**, *105*, 1067.
(72) Farrell, I. R.; Matousek, P.; Kleverlaan, C. J.; Vlček, A., Jr. *Chem.—Eur. J.* **2000**, *6*, 1386.
(73) Gabrielsson, A.; Blanco-Rodríguez, A. M.; Matousek, P.; Towrie, M.; Vlček, A., Jr. *Organometallics* **2006**, *25*, 2148.
(74) Blanco-Rodríguez, A. M.; Towrie, M.; Sýkora, J.; Záliš, S.; Vlček, A. *Inorg. Chem.* **2011**, in press.
(75) Kaim, W. *J. Am. Chem. Soc.* **1982**, *104*, 3883.